

Iterative versus adaptive equalizers in time-variant channels

Clemens Buchacher, Joachim Wehinger

Infineon Technologies AG

81726 München, Germany

Email: {clemens.buchacher,joachim.wehinger}@infineon.com

Mario Huemer

Klagenfurt University

9020 Klagenfurt, Austria

Email: mario.huemer@ieee.org

Abstract—This paper discusses the application of iterative versus adaptive equalizers to a Universal Mobile Telecommunications System (UMTS) High Speed Downlink Packet Access (HSDPA) receiver. Among the investigated algorithms are the Least Mean Square (LMS) and Recursive Least Square (RLS) algorithms and their adaptations to Code Division Multiple Access (CDMA), such as Griffith’s algorithm, as well as the conjugate gradient (CG) algorithm. We show that adaptive algorithms do not perform well in HSDPA scenarios at medium to high mobile speed, and that the conjugate gradient algorithm achieves higher performance at the same or even lower complexity than any of the investigated adaptive algorithms. We also discuss the necessity to consider oversampling.

Index Terms—UMTS, HSDPA, LMMSE, Least Mean Square, LMS, Recursive Least Square, RLS, Griffith, Conjugate Gradient, Oversampling, Regularization, Polyphase.

I. INTRODUCTION

Signals transmitted over a multipath channel to a mobile receiver are subject to interference and fading. In order to achieve the data rates required by services such as HSDPA reliably, the equalizer attempts to reverse the effects of the multipath channel. The most common approach is the Linear Minimum Mean Square Error (LMMSE) equalizer. In order to reduce computational complexity, however, various authors [1]–[5] suggest the use of adaptive equalizers which only approximate the LMMSE equalizer.

We will show in this paper that adaptive equalizers are not well suited for an HSDPA receiver, both in terms of performance and complexity. To support these claims we apply adaptive and iterative equalizer algorithms to a practical system. This raises several issues such as ill-conditioning, synchronization error, and limited equalizer update rate. Our results will show that the conjugate gradient method is superior to LMS and RLS in terms of performance as well as complexity even at low speeds.

A training-based version of the conjugate gradient algorithm has been compared to LMS and RLS by Chowdhury et al. [6]. The training-based approach suffers from adaptation noise, as evidenced by the large number of training symbols required for the investigated algorithms to converge. Contrary to [1], [6] we consider fast fading scenarios, which require algorithms based on channel estimates. We also show that the adaptive CG is inferior to its restarted version at high speeds.

Section II introduces the model used to describe the multipath channel and the LMMSE equalizer. Section III introduces the equalizer algorithms investigated in this paper. Section IV discusses the implications of pulse shaping and oversampling or lack thereof. The simulation environment and results are discussed in Section V.

Notation

We use lower-case bold face variables (\mathbf{a} , \mathbf{b} , \mathbf{c} , ...) to denote vectors and upper-case bold face variables (\mathbf{A} , \mathbf{B} , \mathbf{C} , ...) to denote matrices, \mathbb{Z} to denote the set of integers, \mathbf{I}_n to denote the $n \times n$ unit matrix, $\mathbf{0}_{m,n}$ to denote the $m \times n$ zero matrix. Indices will be omitted where the format is clear from context. We further use $(\cdot)^T$ to denote transposition, $(\cdot)^H$ to denote conjugate transposition, $(\cdot)^*$ to denote complex conjugation, $\|\cdot\|_2$ to denote the 2-norm, and $E(\cdot)$ to denote expectation.

II. SYSTEM MODEL

We consider the received signal

$$y(N_p n + p) = \sum_{l=0}^{L-1} h_{N_p l + p}(n) s(n - l + L - 1) + v(N_p n + p)$$

for $p = 0, \dots, N_p - 1, n \in \mathbb{Z}$, where s is the chip-rate transmit signal, v is a complex Gaussian noise process, and $h_k, k = 0, \dots, LN_p - 1$ denotes the k th delay element of the N_p times oversampled multipath channel impulse response. L denotes the length of the multipath channel impulse response.

We will assume that h_k is constant for intervals of the equalizer length Q , i.e., $|h_k(n) - h_k(n + m)|$ is negligible for $m = 0, 1, \dots, Q - 1$ for all $n \in \mathbb{Z}$. We can therefore define the vector representation of the received signal

$$\mathbf{y}(n) = \mathbf{H}(n)\mathbf{s}(n) + \mathbf{v}(n) \quad \text{for } n \in \mathbb{Z}, \quad (1)$$

where

$$\begin{aligned} \mathbf{y}(n) &= [y(N_p(n + 1) - 1), \dots, y(N_p(n - Q + 1))]^T, \\ \mathbf{v}(n) &= [v(N_p(n + 1) - 1), \dots, v(N_p(n - Q + 1))]^T, \\ \mathbf{s}(n) &= [s(n + L - 1), \dots, s(n - Q + 1)]^T, \end{aligned}$$

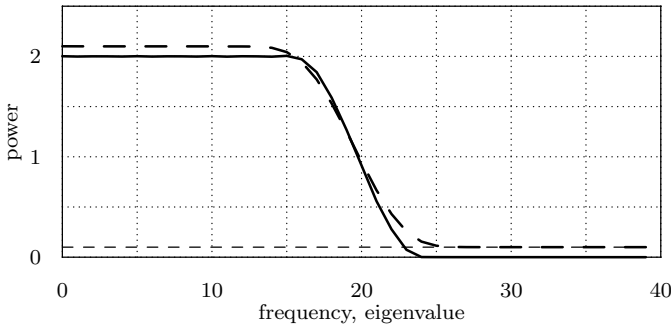


Fig. 1. Raised cosine spectrum (—) and eigenvalue distribution λ (---) of the corresponding autocorrelation matrix with regularization factor η (· · · ·).

and

$$\mathbf{H} = \begin{bmatrix} \mathbf{h}_0 & \mathbf{h}_1 & \cdots & \mathbf{h}_{L-1} & \mathbf{0} & \cdots & \mathbf{0} \\ \mathbf{0} & \mathbf{h}_0 & \cdots & & \mathbf{h}_{L-1} & \ddots & \vdots \\ \vdots & \ddots & \ddots & & & \ddots & \mathbf{0} \\ \mathbf{0} & \cdots & \mathbf{0} & \mathbf{h}_0 & \cdots & \cdots & \mathbf{h}_{L-1} \end{bmatrix}$$

is the $N_p Q \times Q + L - 1$ channel convolution matrix, where

$$\mathbf{h}_l = [h_{N_p(l+1)-1}, \dots, h_{N_p l}]^T$$

for $l = 0, \dots, L - 1$. We will sometimes drop the index n for notational convenience, but it is understood implicitly that the channel and variables derived from it are functions of the time index n .

Note that the channel impulse response describes the multipath channel as observed by the receiver. It includes the transmit and receive pulse shaping filters. UMTS has a root raised cosine (RRC) pulse shape with a spectrum as depicted in Figure 1. For the same reason, the noise process v is colored.

The transmit chip sequence is actually a superposition of spread and scrambled UMTS and HSDPA channels. Due to scrambling, the transmit chips are mutually uncorrelated, i.e., $E(\mathbf{s}\mathbf{s}^H) = \mathbf{I}$. It is therefore possible to disregard the CDMA specific properties of the transmit signal in order to treat equalization entirely at the chip-level.

III. EQUALIZER ALGORITHMS

The desired transmit chip $d = s(n) = \mathbf{e}_L^T \mathbf{s}$, where \mathbf{e}_n denotes a column vector with a one at index n and zeros otherwise, is estimated using the linear combination of receive samples $\hat{d} = \mathbf{w}^H \mathbf{y}$. Each of the following equalizer algorithms approximates \mathbf{w} such that the mean square $J(\mathbf{w}) = E(|e|^2)$ of the error $e = d - \hat{d}$ is minimized. If the statistics of \mathbf{y} and d are known, this criterion is satisfied by the *Wiener solution* [7]

$$\mathbf{w}_{\text{LMMSE}} = \mathbf{C}_y^{-1} \mathbf{c}_{yd}, \quad (2)$$

where $\mathbf{C}_y = E(\mathbf{y}\mathbf{y}^H) = \mathbf{H}\mathbf{H}^H + \mathbf{C}_v$, $\mathbf{C}_v = E(\mathbf{v}\mathbf{v}^H)$ and $\mathbf{c}_{yd} = E(\mathbf{y}d^*) = \mathbf{H}\mathbf{e}_L$. The corresponding equalizer is known as the LMMSE equalizer.

Since the channel is not stationary, the algorithms discussed in the following sections process blocks of R receive samples

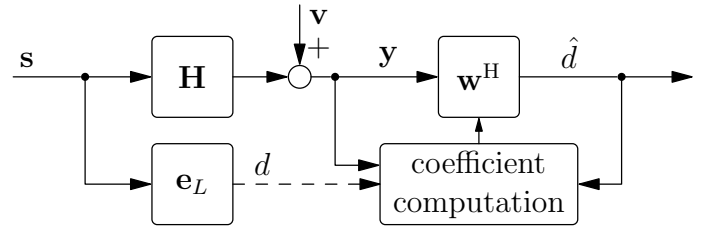


Fig. 2. Multipath channel, equalizer and coefficient computation.

during which the channel is approximated to be constant. The channel state is estimated for each block and the corresponding equalizer weight vector $\mathbf{w}(m)$ is applied to the input vectors $\mathbf{y}(n), \mathbf{y}(n+1), \dots, \mathbf{y}(n+R-1)$ for $n = mR$. Since the received signal is filtered with the equalizer weight vector at the chip rate, independently of the considered algorithm, complexity comparisons will consider only coefficient computation complexity.

In the following sections we discuss the training-based LMS and RLS algorithms, as well as their channel estimation based versions, and the conjugate gradient algorithm. A generic diagram for these algorithms is shown in Figure 2.

A. Least Mean Square and Griffith's Algorithm

The Least Mean Square (LMS) algorithm successively approximates the Wiener solution by adapting the weight vector in the direction of the error gradient. In order to compute the error gradient, the autocorrelation matrix \mathbf{C}_y and cross-correlation vector \mathbf{c}_{yd} are approximated by their instantaneous counterparts $\mathbf{y}\mathbf{y}^H$ and $\mathbf{y}d^*$.

Performance of the LMS algorithm applied to HSDPA is poor, because the training chip sequence amounts to only one tenth of the total signal power [2]. The cross-correlation vector \mathbf{c}_{yd} , however, can be estimated by correlating the received signal with the training chip sequence. The low complexity of channel estimation allows correlation at the chip rate and therefore has greater accuracy. The channel estimator is discussed in Section V. Note that the performance achieved by [6] can not be compared, because they simulate a stationary channel.

By substituting $\mathbf{y}d^*$ with its statistical average $\mathbf{c}_{yd} = E(\mathbf{y}d^*)$ we obtain Griffith's algorithm [1]–[4], which does not require knowledge of the transmit chip d . Note that Griffith's algorithm requires normalization in fast fading scenarios [3].

Algorithm 1 – Griffith

Initialization: $\mathbf{w} = \mathbf{0}$

$$\mathbf{w} \leftarrow \mathbf{w} + \mu \frac{\mathbf{c}_{yd} - \mathbf{y}\hat{d}^*}{\mathbf{y}^H \mathbf{y}}$$

The choice of the step size parameter μ is a tradeoff between adaptation noise and convergence speed. The complexity of Griffith's algorithm is equal to $2QN_p/R$ complex multiply accumulate (MAC) operations.

B. Recursive Least Squares

The Recursive Least Squares (RLS) algorithm has been shown to increase convergence speed of the LMS algorithm [8]. It applies the matrix inversion lemma to the recursive equation

$$\begin{aligned}\Phi(0) &= \delta \mathbf{I} \\ \Phi(m) &= \lambda \Phi(m-1) + \mathbf{y}(mR) \mathbf{y}^H(mR) \\ &= \sum_{i=1}^m \lambda^{m-i} \mathbf{y}(iR) \mathbf{y}^H(iR) + \delta \lambda^m \mathbf{I}\end{aligned}$$

for an exponentially weighted average of the instantaneous autocorrelation $\mathbf{y} \mathbf{y}^H$ in order to obtain an approximation $\mathbf{P} = \Phi^{-1}$ of the inverse autocorrelation matrix \mathbf{C}_y^{-1} [8]. The exponential weighting factor λ , $0 < \lambda < 1$ controls the adaptation speed in analogy to the step size parameter μ . We define $\mu := 1 - \lambda$ in order to emphasize the close relationship to the corresponding parameter of the LMS algorithm. The parameter δ regularizes Φ for the initial steps, at which point the estimation variance is large and could easily cause instability.

Again, when applied to HSDPA this algorithm's performance is poor, because only one tenth of the transmit signal power is available for training. In analogy to Griffith's algorithm, the weight update rule for the RLS algorithm using the cross-correlation vector becomes [4], [5]

$$\mathbf{w} \leftarrow \mathbf{w} + \alpha \mathbf{P} (\mathbf{c}_{y_d} - \mathbf{y} \hat{d}^*).$$

But the recursive update is now superfluous, since \mathbf{P} already approximates the inverse of \mathbf{C}_y so that \mathbf{w} can be computed directly using Equation 2. The resulting modified RLS updates \mathbf{w} using the following algorithm.

Algorithm 2 – Correlating Recursive Least Squares

Initialization: $\mathbf{P} = \delta^{-1} \mathbf{I}$
 $\mathbf{p} \leftarrow \mathbf{P} \mathbf{y}$
 $\beta \leftarrow 1 / (\lambda + \mathbf{y}^H \mathbf{p})$
 $\mathbf{w} \leftarrow (1 - \lambda)^{-1} \mathbf{P} \mathbf{c}_{y_d}$
 $\mathbf{P} \leftarrow \lambda^{-1} (\mathbf{P} - \beta \mathbf{p} \mathbf{p}^H)$

We denote this the Correlating RLS (CRLS) algorithm. The factor $(1 - \lambda)^{-1}$ compensates for the fact that

$$\mathbb{E}(\Phi) = \frac{1 - \lambda^m}{1 - \lambda} \mathbf{C}_y + \delta \lambda^m \mathbf{I} \xrightarrow{m \rightarrow \infty} (1 - \lambda)^{-1} \mathbf{C}_y.$$

The CRLS algorithm's complexity is equal to $(2.75(QN_p)^2 + 1.5QN_p)/R$ MACs. The update of \mathbf{w} requires an extra matrix-vector multiplication compared to the classical RLS. Note that "Fast RLS" algorithms with linear complexity exist. They exploit the fact that the vector $\mathbf{y}(n+1)$ is a shifted version of $\mathbf{y}(n)$ with only N_p new samples at each step n . This optimization is not applicable here, because \mathbf{w} is not updated for each n , but only for each $m = Rn$ [5].

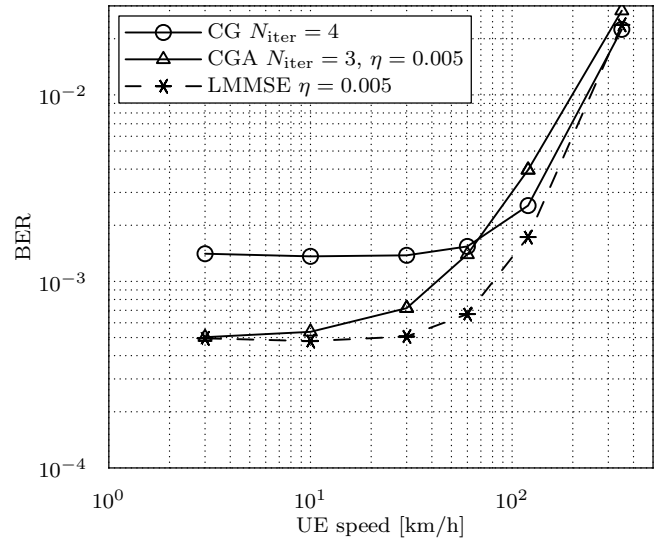


Fig. 3. BER performance of conjugate gradient with starting value 0 (CG) and with previous starting value (CGA) for low and high speeds, SNR = 20 dB, Vehicular A power delay profile, and ideal channel estimation, update rate $R = 1280$.

C. Conjugate Gradient Algorithm

The conjugate gradient algorithm is an iterative method similar to gradient descent, but instead of searching in the direction of residual error, it moves in mutually "conjugate" directions to increase convergence speed.

The following procedure solves Equation 2 for $\mathbf{A} := \mathbf{C}_y + \eta \mathbf{I}$, $\mathbf{b} := \mathbf{c}_{y_d}$ and $\mathbf{x} := \mathbf{w}$. Contrary to previous sections, the Wiener solution is computed based solely on \mathbf{C}_y and \mathbf{c}_{y_d} . The regularization factor η will be explained in Section IV.

Algorithm 3 – Conjugate Gradient

Initialization: $\mathbf{x} = \mathbf{0}$
 $\mathbf{r} \leftarrow \mathbf{b} - \mathbf{A} \mathbf{x}$
 $k \leftarrow 0$
while $k < N_{\text{iter}}$ and $\|\mathbf{r}\|_2^2 > 0$ **do**
 if $k = 0$ **then**
 $\mathbf{p} \leftarrow \mathbf{r}$
 else
 $\beta \leftarrow \|\mathbf{r}\|_2^2 / \|\mathbf{r}_{\text{old}}\|_2^2$
 $\mathbf{p} \leftarrow \mathbf{r} + \beta \mathbf{p}$
 end if
 $\beta \leftarrow \|\mathbf{r}\|_2^2 / (\mathbf{p}^H \mathbf{A} \mathbf{p})$
 $\mathbf{x} \leftarrow \mathbf{x} + \beta \mathbf{p}$
 $\mathbf{r}_{\text{old}} \leftarrow \mathbf{r}$
 $\mathbf{r} \leftarrow \mathbf{r} - \beta \mathbf{A} \mathbf{p}$
 $k \leftarrow k + 1$
end while

The initial residual \mathbf{r} is equal to \mathbf{b} if we use the starting value $\mathbf{x} = \mathbf{0}$. Alternatively, it is possible to reuse the previous solution. We denote this alternative *adaptive CG* or CGA. The cost of computing the initial residual $\mathbf{r} = \mathbf{b} - \mathbf{A} \mathbf{x}$ for a non-zero starting value is close to an entire iteration, however. If channel fading is fast with respect to the equalizer update

rate, an extra iteration is more beneficial than starting with the solution for the previous channel state. This tradeoff is shown in Figure 3.

The CG algorithm requires up to $N_p Q$ iterations in order to compute the Wiener solution exactly, but it converges to a very accurate solution after as few as 4 iterations. The total complexity evaluates to $N_{\text{iter}}((QN_p)^2 + 2.5QN_p)$ MACs for the CG algorithm, plus an extra $(QN_p)^2$ MACs for the CGA algorithm.

IV. OVERSAMPLING

Some publications investigate a system without oversampling [4], [6] or without even pulse shaping [2], [3], [5], which lends itself to many simplifications. For example, \mathbf{C}_y is Toeplitz. The Toeplitz structure also enables algorithms such as the Prefilter Rake [2], which relies on the fact that the inverse autocorrelation matrix is approximately Toeplitz. The same is not true in the block Toeplitz case, which occurs if the received signal is oversampled. A T-spaced equalizer, i.e. an equalizer without oversampling, on the other hand, is highly sensitive to synchronization. If timing is unfavorable, the receiver incurs significant performance degradation due to aliasing. The performance of the T-spaced and T/2-spaced LMMSE equalizer for Rayleigh fading with frequency flat and Pedestrian B power delay profiles is plotted over timing offset in Figure 4. For frequency flat fading, timing offset can be removed using interpolation, but for power delay profiles such as Pedestrian B there is no correct timing. For this reason, the T-spaced equalizer is not considered in this paper.

Even if the sampling time is synchronized, systems that do and systems that do not model pulse shaping cannot be compared. Figure 5a shows the performance results for a system without oversampling and pulse shaping. The performance gap between LMMSE and CRLS is much smaller compared to Figure 5b, where oversampling and pulse shaping are modelled correctly. Figure 5a misleadingly indicates good performance of the CRLS algorithm. It is therefore not sufficient to consider the system without oversampling and pulse shaping. Subsequent simulation results correspond to a system with oversampling ratio $N_p = 2$.

The simulation results for $N_p = 1$ and $N_p = 2$ are different, because the oversampled system is *ill-conditioned*. The signal spectrum has zero power outside the RRC pulse bandwidth, which becomes visible due to oversampling. As a consequence of the Grenander and Szegö Grenander theorem [9] the eigenvalue distribution of \mathbf{C}_y is similar to the power spectrum of \mathbf{y} . This similarity is illustrated in Figure 1, which shows the positive half of the RRC power spectral density, as well as the eigenvalues of the corresponding autocorrelation matrix, sorted in descending order.

Consider the regularization factor η added to the diagonal of the autocorrelation matrix \mathbf{C}_y . It essentially imitates a small additive white noise signal. Figure 1 shows that the regularization factor η causes an offset in the eigenvalue distribution. This fact becomes immediately apparent from the eigenvalue decomposition $\mathbf{C}_y + \eta\mathbf{I} = \mathbf{U}(\Lambda + \eta\mathbf{I})\mathbf{U}^H$, where

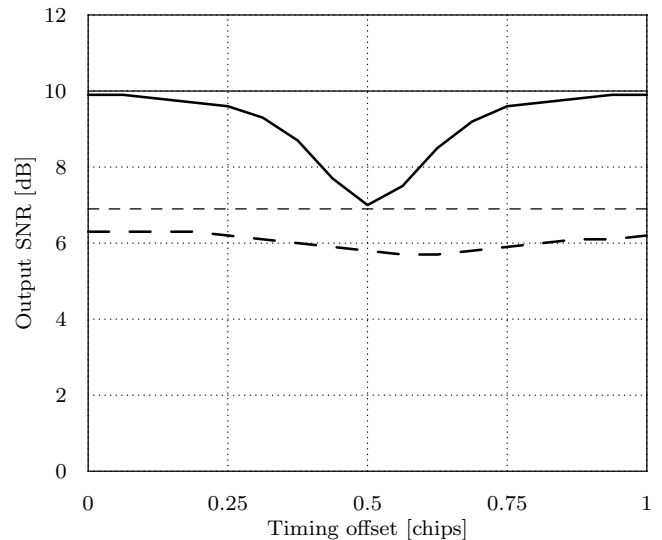


Fig. 4. T-spaced frequency flat (—), Pedestrian B (---) vs. T/2-spaced frequency flat (---), Pedestrian B (---) equalizer output SNR over timing offset, $N_p = 2$, Rayleigh fading, SNR = 10 dB, ideal channel estimation and coefficient computation.

\mathbf{U} is unitary and Λ is a diagonal matrix the entries of which are the eigenvalues λ_i of \mathbf{C}_y . Regularization allows to give an upper bound for the condition number $\kappa = \frac{\max\{\lambda_i\} + \eta}{\min\{\lambda_i\} + \eta} \leq \frac{\max\{\lambda_i\}}{\min\{\lambda_i\}} + 1$. If no regularization is employed, the system is *ill-conditioned*, because $\min\{\lambda_i\}$ is arbitrarily small. This has several undesirable consequences. For instance, the eigenvalue spread negatively affects convergence speed and stability of the LMS and RLS algorithms. The LMS algorithm is stable if $\mu < 2/\|\mathbf{C}_y\|_2$, but ill-conditioning can cause the RLS algorithm to become unstable even for small step sizes. Since the autocorrelation matrix is not used directly the RLS algorithm is regularized by adding an artificial white noise signal to the receive samples. Note that this is in addition to the regularization parameter δ , which is only relevant during the initialization steps. The CRLS algorithm is particularly prone to instability. It requires a regularization factor of at least $\eta = 0.01$. Unfortunately, regularization also causes a noise floor and therefore degrades performance at high SNR.

The problem of ill-conditioning can be avoided entirely by equalizing each polyphase $\mathbf{y}^{(p)}(n) = [y(N_p n + p), y(N_p(n-1) + p), \dots, y(N_p(n-Q+1) + p)]^T$ separately and combining the results of all polyphase equalizers. Using this approach, the CRLS algorithm can be used without regularization. The corresponding polyphase algorithm is denoted PCRLS. It approximates the T-spaced LMMSE solution using the CRLS algorithm for each polyphase, i.e.,

$$\mathbf{w}_{\text{LMMSE}}^{(p)} = \mathbf{C}_{\mathbf{y}^{(p)}}^{-1} \mathbf{c}_{\mathbf{y}^{(p)}} \quad \text{for } p = 0, \dots, N_p - 1.$$

The individual equalizer outputs are subsequently combined to give the joint estimate $\hat{d} = \frac{1}{N_p} \sum_{i=1}^{N_p} \mathbf{w}_{\text{LMMSE}}^{(p)H} \mathbf{y}^{(p)}$.

Not all algorithms require regularization. For example, since the conjugate gradient algorithm uses only 4 iterations, it achieves the same effect implicitly [10]. The same is not true

| Pedestrian B | | Vehicular A | |
|------------------|------------|------------------|------------|
| Delay [μ s] | Power [dB] | Delay [μ s] | Power [dB] |
| 0.0 | 0.0 | 0.0 | 0.0 |
| 0.2 | -0.9 | 0.31 | -1.0 |
| 0.8 | -4.9 | 0.71 | -9.0 |
| 1.2 | -8.0 | 1.09 | -10.0 |
| 2.3 | -7.8 | 1.73 | -15.0 |
| 3.7 | -23.9 | 2.51 | -20.0 |

TABLE I
POWER DELAY PROFILES [11].

for the CGA algorithm, because it effectively computes the exact Wiener solution for sufficiently low speeds. Furthermore, for the reasons discussed above, regularization is only an issue if $N_p > 1$.

V. SIMULATION RESULTS

Judging from the power delay profiles defined in HSDPA standard testcase specifications [11], typical channels of interest have up to 5μ s excess delay spread, which at the UMTS chip rate of 3.84 MHz corresponds to approximately $L = 20$ chips. The equalizer length $Q = 20$ is matched to the channel length.

The simulation scenario corresponds to the HSDPA standard testcases defined in [11]. Other cell interference is modelled as white Gaussian noise. Noise samples in this model are band limited due to receive pulse shaping, however.

The HSDPA simulator uses QPSK modulation, 5 High Speed Physical Downlink Shared Channel (HS-PDSCH) multicodes with spreading factor 16 each, $P_{\text{HS-PDSCH}} = -3$ dB HS-PDSCH power and $P_{\text{CPICH}} = -10$ dB Common Pilot Channel (CPICH) power. The remaining transmit power P_{OCNS} is filled with the Orthogonal Channel Noise Simulator (OCNS) signal. Bit error rate is plotted in Figures 5a, 5b and 6 for the *Pedestrian B* and *Vehicular A* power delay profiles at 3 km/h and 30 km/h, respectively. The power delay profiles are reproduced in Table I.

The channel is estimated by correlating the received signal with the $N = 256$ chip length CPICH symbol. In order to reduce channel estimation error, the correlator output is fed to a low pass filter of first order with transfer function

$$F(z) = \frac{\alpha}{1 + (1 - \alpha)z^{-1}},$$

where $\alpha = 0.05$ for 3 km/h, and $\alpha = 0.2$ for 30 km/h speed.

After equalization, the signal is descrambled and despread. The bit error rate is evaluated from hard decisions at the symbol demapper output. For simplicity, throughput is not considered. However, since HSDPA supports adaptive modulation and coding, the system can take advantage of improved equalizer performance regardless of the operating point. Simulation statistics are recorded only after the weight vector has converged such that the weight error $\|\mathbf{w} - \mathbf{w}_{\text{LMMSE}}\|_2^2 / (QN_p)$ is less than 0.01. The simulation stop criterion is 40000 slots¹ at 3 km/h, 20000 at 10 km/h, 10000 at 30 km/h and 5000

¹One slot corresponds to 2560 transmit chips or 0.67 ms.

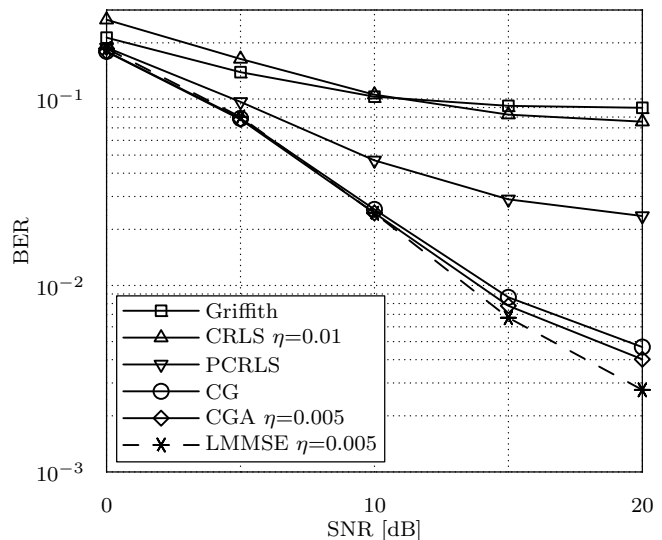


Fig. 6. Bit error rate performance for Vehicular A power delay profile at 30 km/h mobile speed.

TABLE II
OPTIMIZED SIMULATION PARAMETERS.

| Algorithm | Parameters |
|-----------|--|
| (P)CRLS | $\mu = 5 \cdot 10^{-3}$ $\lambda = 1 - \mu$ $\delta = \mu$ $R = 64$ chips |
| Griffith | $\mu = 0.05$ at 3 km/h $\mu = 0.1$ at 30 km/h $R = 16$ chips |
| CG | $N_{\text{iter}} = 4$ $R = 1280$ chips |
| CGA | $N_{\text{iter}} = 3$ $R = 1280$ chips |
| LMMSE | $R = 1280$ chips |

for 60 km/h or more. Also, simulation is stopped only after a minimum of 1000 bit errors. The remaining simulation parameters were optimized empirically and are summarized in Table II.

The “LMMSE algorithm” computes the Wiener solution exactly, but uses real channel estimation. It shows the performance that could be achieved if a direct solver were used instead of the conjugate gradient algorithm.

In Figure 5b, only the conjugate gradient based algorithms approach LMMSE equalizer performance in the range between 0 and 10 dB SNR. At higher speeds, Figure 6 shows that the adaptive algorithms’ performance deteriorates even further, while the CG algorithm is still close to LMMSE equalizer performance despite its much lower update rate. These results suggest that even at the cost of error due to a lower update rate, it is better to compute the Wiener solution iteratively, than to update the equalizer coefficients more frequently at the cost of adaptation noise. From Figure 3 it becomes apparent, that at about 60 km/h and beyond, the adaptive CG performs worse than the plain CG algorithm.

The number of complex multiply accumulate (MAC) operations per chip is shown in Figure 7. Due to their quadratic

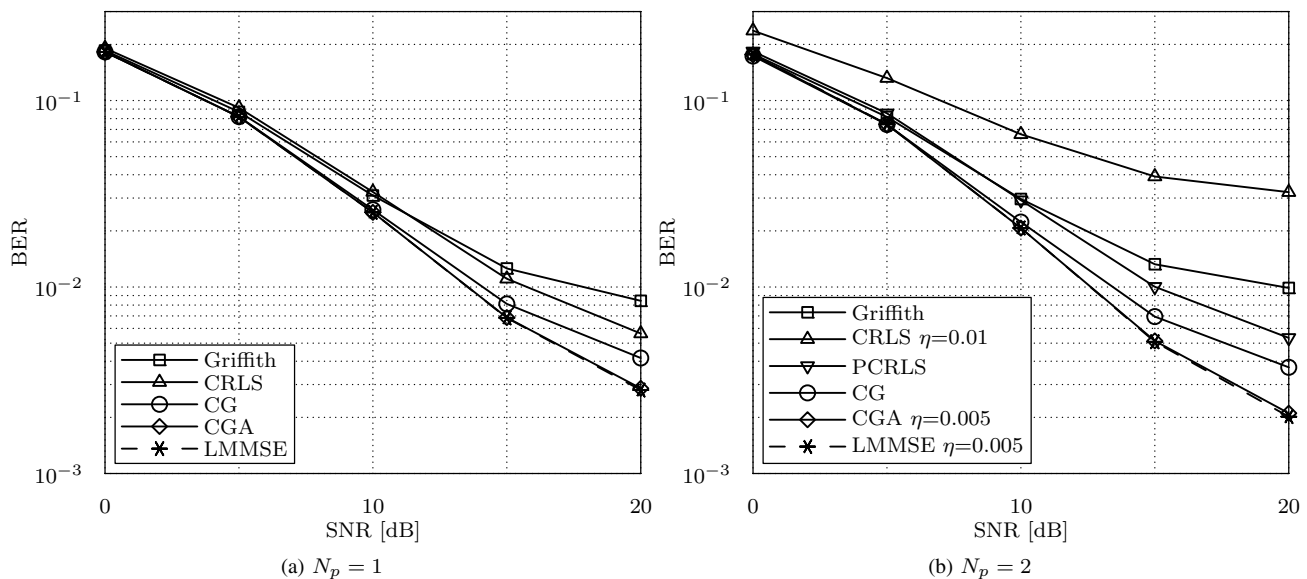


Fig. 5. Bit error rate performance for Pedestrian B power delay profile at 3 km/h mobile speed.

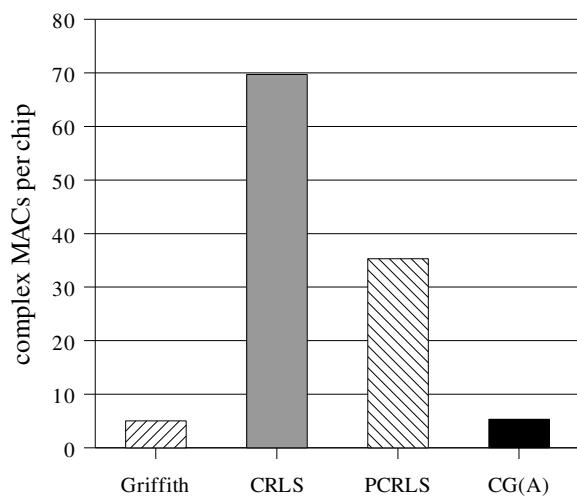


Fig. 7. Approximate number of operations for $Q = 20$, $N_{\text{iter}} = 4$.

complexity and high update rate, RLS based algorithms have much greater complexity than Griffith's algorithm or even the CG algorithm. In fact, the CG algorithm is on par even with Griffith's algorithm despite its quadratic complexity, because it has a much lower update rate.

VI. CONCLUSION

The LMS and RLS algorithms are commonly considered to be low-complexity alternatives to direct LMMSE equalizer coefficient computation. In order to employ these algorithms in a CDMA system, however, they have to be modified to work with code-multiplexed training signals. We have shown that these modified algorithms suffer a performance hit compared to the optimum LMMSE equalizer at high SNR, as well as high mobile speeds. It was shown that oversampling is required

to guarantee reliable performance at fractional multipath delays.

The conjugate gradient algorithm, in particular its adaptive version, was shown to achieve performance close to the optimum LMMSE equalizer for high SNR as well as high mobile speeds. Furthermore, thanks to its fast convergence and low update rate, the conjugate gradient algorithm has computational complexity similar to the Griffith algorithm.

REFERENCES

- [1] L. Mailaender, "Linear MIMO Equalization for CDMA Downlink Signals With Code Reuse," *IEEE Trans. Wireless Comm.*, vol. 4, no. 5, pp. 2423–2434, 2005.
- [2] K. Hooli, M. Juntti, M. J. Heikkilä, P. Komulainen, M. Latva-aho and J. Lilleberg, "Chip-Level Channel Equalization in WCDMA Downlink," *EURASIP J. Appl. Signal Process.*, no. 1, pp. 767–770, 2002.
- [3] J. Karlsson and H. Imai, "Improved Single-User Detector for WCDMA Systems based on Griffiths' Algorithm," *IEEE 52nd Vehicular Tech. Conf.*, vol. 5, pp. 2352–2359, 2000.
- [4] O. Prátor, C. Unger, A. Zoch and G. P. Fettweis, "Performance of Adaptive Chip Equalization for the WCDMA Downlink in Fast Changing Environments," *IEEE 7th Int. Symp. Spread-Spectrum Techn. & Appl.*, vol. 1, pp. 273–277, Prague, Czech Republic, Sept. 2–5, 2002.
- [5] D. Morgan, "An Adaptive RLS MIMO Equalizer Algorithm for HS-DPA," *40th Asilomar Conf. on Signals, Systems and Computers*, pp. 1016–1021, 2006.
- [6] S. Chowdhury, M. D. Zoltowski, "Application of Conjugate Gradient Methods in MMSE Equalization for the Forward Link of DS-CDMA," *54th Vehicular Technology Conference*, vol. 4, pp. 2434–2438, Atlantic City, NJ, USA, 2001.
- [7] S. M. Kay, *Fundamentals of Statistical Signal Processing*, Prentice Hall, 1993.
- [8] S. Haykin, *Adaptive Filter Theory*, Prentice Hall, 3rd Edition, 1996.
- [9] R. H. Chan and M. K. Ng, *Conjugate Gradient Methods for Toeplitz Systems*, 1994.
- [10] M. Hanke, *Conjugate gradient type methods for ill-posed problems*. Pitman Research Notes in Mathematics Series, Longman House, Harlow, Essex, 1995.
- [11] 3rd Generation Partnership Project, *Technical Specification 25.101; User equipment (UE) radio transmission and reception (FDD)*, V8.2.0, Release 8, 2008.